Contents list available http://www.kinnaird.edu.pk/

Journal of Natural and Applied Sciences Pakistan

Journal homepage: http://jnasp.kinnaird.edu.pk/

IN SILICO ANALYSIS AND HOMOLOGY MODELING OF Ω-CONOTOXIN FROM SELECTED PISCIVOROUS SPECIES

Noel A. Saguil[2,] Cristine Anne B. Comia[2,] Arial Joy J. Roderos[1] Rachel Joy S. Ellorin[1], Jimiwell R. Bernabe[1*,] Marian Jeremy D. Aggabao[1], Lenn Rose N. Cawaling[1], Elijsha Meari A. Gabriel[1], Arlene N. Naca, Jacob Israel C. De Asis[2], Analette M. Guinto[1,2], and Alvin N. Caril1,[2]
[1]Graduate School, Polytechnic University of the Philippines, Sta. Mesa, Manila
[2]Department of Biology, Polytechnic University of the Philippines, Sta. Mesa, Manila

Article Info

*Corresponding Author
Email: bernabejimiwell@gmail.com

Abstract

Cone snails (genus Conus) are recognized as some of the most venomous marine mollusks, utilizing specialized venom to capture prey such as fish, worms, and other mollusks. This venom comprises a diverse array of bioactive peptides collectively called conotoxins. Conotoxins are small, disulfide-rich peptides that exhibit high specificity for various components of neural transmission, targeting ion channels and receptors critical to neuronal function. Due to their precise mode of action, conotoxins present significant potential for pharmacological applications and drug development. Despite this potential, the structural characterization of conotoxins remains limited, creating gaps in our understanding of their affinities and specificities. This study employs computational (in silico) analysis and homology modeling to investigate the physicochemical properties, structural domains, and conformations of ω-conotoxins derived from select piscivorous Conus species. The results indicate considerable variability in the protein lengths of ω-conotoxins. Notably, all examined ω-conotoxins possess isoelectric points exceeding 7.0, indicating a strongly alkaline nature. Additionally, the stability indices of these conotoxins demonstrate variability, with some exhibiting stability while others are classified as unstable. The aliphatic index of the identified conotoxins ranges from 27.93 to 105.40, suggesting substantial stability across a diverse temperature range. GRAVY values for ω-conotoxins range from -0.921, demonstrating high hydrophilicity (exemplified by ω-conotoxin MVIIC), to 0.073, reflecting high hydrophobicity (illustrated by ω-conotoxin CVID). Most ω-conotoxins are categorized within the omega-conotoxin domain, with Pfam PF02950 and PROSITE PS60004 patterns serving as common motifs across species. The analysis of secondary structures reveals that random coils are the predominant structural configuration, followed by alpha-helices, beta-strands, and beta-turns. Ultimately, the projected models for ω-conotoxins MVIIC, MVIIB, TVIA, CVIA, CVIC, CVIB, and CVIF demonstrate high structural quality, with over 90% of their residues residing within favored regions of the Ramachandran plot.

Keywords

In silico analysis, homology modeling, ω-conotoxin, piscivorous species, voltage-gated calcium channels

1. Introduction

Cone snails, members of the family Conidae, are ecologically significant marine gastropods known for their potent venom composed of conotoxins, which are small, disulfide-rich peptides with high pharmacological potential (Puillandre *et al*., 2014; Hendricks, 2018; Olivera *et al*., 1985; Jin *et al*., 2019). While these venoms primarily serve for predation by inducing rapid paralysis, their remarkable diversity and molecular specificity highlight their biomedical importance. With numerous estimated unique conotoxins across species, many remain structurally uncharacterized, limiting our understanding of their therapeutic potential. Conducting this study is crucial, as in silico analysis and homology modeling can determine structural features that may inform drug discovery and biomedical applications. Each species within the genus *Conus* produces a distinctive venom composition that can vary depending on ecological context and whether the venom is being utilized for predation or defense (Dutertre *et al*., 2014; Robinson *et al*., 2014). The molecular diversity of these venoms is of high magnitude, as they can act on a broad spectrum of molecular targets, including ion channels, G-protein coupled receptors (GPCRs), neurotransmitter transporters, and various enzymes (Olivera, 2006; Robinson *et al*., 2014; Jin *et al*., 2019). Their remarkable abundance, combined with their small size, structural stability, and highly selective molecular interactions, has made conotoxins invaluable in biomedical research and drug discovery. Their ability to precisely modulate specific targets not only provides tools for probing neurophysiological processes but also highlights their potential as therapeutic leads (Becker & Terlau, 2008). Conotoxins are categorized into distinct superfamilies based on sequence homology, cysteine framework patterns, and functional activities (Olivera, 2006). Among these, omega-conotoxins are particularly notable for their potent inhibition of voltage-gated calcium channels (VGCCs), which are critical in controlling neurotransmitter release and muscle contraction in vertebrates (Hannon & Atchison, 2013). The evolutionary refinement of omega-conotoxins is especially apparent in piscivorous cone snail species, which have adapted their toxins to target VGCCs in fish with remarkable specificity and potency (Oliver, 2006). By blocking calcium ion entry at presynaptic terminals, ω-conotoxins disrupt synaptic transmission and induce rapid paralysis in prey. These precise mechanisms have also made ω-conotoxins indispensable as molecular probes for studying calcium channel physiology and promising candidates in the development of novel analgesics, given their established role in modulating pain pathways (Altier *et al*., 2007; Hannon & Atchison, 2013). Despite the identification of numerous ω-conotoxin variants, many structural features and the nature of their interactions with different VGCC subtypes remain incompletely characterized. A deeper understanding of these structural determinants is necessary for informing the rational design of new therapeutics targeting calcium channels

implicated in chronic pain, epilepsy, and neurodegenerative disease. The present study, therefore, applies in silico approaches, specifically physicochemical analysis with homology modeling, to investigate ω-conotoxins derived from selected piscivorous cone snail species. The search for novel therapeutics increasingly relies on identifying bioactive molecules that modulate biological processes underlying disease (Lage *et al*., 2018). Historically, structural studies of conotoxins have relied heavily on labor-intensive methods such as nuclear magnetic resonance (NMR) spectroscopy and X-ray crystallography (Jin *et al*., 2019). While powerful, these techniques are costly and time-consuming, limiting their scalability. Recent advances in computational biology have made in silico methods an alternative for structural characterization and drug discovery (Sahay *et al*., 2020). Among these, homology modeling has been increasingly utilized, as this technique predicts the three-dimensional structure of a protein based on sequence similarity to experimentally solved structures, enabling efficient structural and functional analysis (Sahay *et al*., 2020; Waterhouse *et al*., 2018). In drug discovery, homology modeling allows researchers to evaluate structural roles within cells, explore protein function, and investigate potential molecular interactions relevant to therapeutic development. In this context, the present study employs computational tools to analyze critical parameters of ω-conotoxins, including domain structures, peptide sequences, and secondary structure. By integrating these analyses with homology modeling, the study aims to provide insights into the structure-function relationships of ω-conotoxins from piscivorous *Conus* species and evaluate their potential as therapeutic leads targeting VGCCs.

2.Methodology

2.1 Retrieval of Target Protein Sequence

Omega-conotoxin protein sequences were selected based on their network structures and functional properties from the National Center for Biotechnology Information (NCBI) database, which integrates sequences from Genbank, RefSeq, TPA, SwissProt, PIR, PRF, and PDB. Additional protein sequences were retrieved from the Universal Protein Resource (UniProt) database (http://www.uniprot.org). Specifically, sequences from *Conus geographus, C. magus, C. tulipa, C. striatus,* and *C. catus* were obtained and saved in PDB format for further analysis. These piscivorous species were selected due to their relevance in investigating the roles of ω-conotoxins in modulating voltage-gated calcium channels.

2.2 Physicochemical Parameter and Characterization

The physicochemical properties of the retrieved sequences were assessed using the ProtParam tool of Expasy. By supplying the UniProtKP accession number to the server, parameters such as molecular weight, theoretical isoelectric point (pI), instability index (II), aliphatic index (AI), and Grand Average of Hydropathicity (GRAVY) were determined.

2.3 Domain Analysis

Domain identification was performed using the InterPro online platform, which integrates the Pfam database. Raw protein sequences were submitted to InterPro, and domains were identified using hidden Markov Models (HMMs) within Pfam, enabling classification of the ω-conotoxins into specific protein families.

2.4 Secondary Structure Prediction

Secondary structural elements were predicted using Self-Optimized Prediction with Method and Alignment (SOPMA), a widely utilized tool for protein structural analysis. SOPMA identified regions likely to form α-helices, β-sheets, β-turns, and random coils. Sequences in PDB format were submitted to the server using default parameters.

2.5 Constructing and Verifying ω-Conotoxin Models

Three-dimensional structural models of ω-conotoxins were generated using different approaches depending on sequence length. For sequences exceeding 30 amino acids, the SWISS-Model Server was utilized, while shorter sequences were modeled using the UCLA-DOE LAB's SAVES server. Model quality was evaluated using Global Model Quality Estimation (GMQE) and Qualitative Model Energy Analysis (QMEAN) scores, where GMQE values closer to 1.0 indicated higher confidence, and QMEAN values below 4.0 supported structural reliability. Following construction, PDB files were submitted to PDBsum server for stereochemical validation. PROCHECK was employed to generate Ramachandran plots, examining the dihedral angles of protein backbone residues. The presence of the majority of residues in favored regions confirmed stereochemical accuracy, thereby validating the reliability of the 3D models for subsequent functional and interaction analyses.

3. Results

3.1 Retrieved Target Protein Sequences

Piscivorous cone snails analyzed in this study include *Conus geographus, C. magus, C. striatus, C. tulipa,* and *C. tulipa*. The protein sequences of ω-conotoxin from these cone snails were obtained from the UniProtKB database and saved in PDB format for further analysis. A total of 16 ω-conotoxins were obtained (two from *C. geographus*, four from *C. magus*, three from *C. striatus*, one from *C. tulipa*, and five from *C. tulipa*). Sequence lengths of each ω-conotoxin were recorded, which range from 25 to 73. Examination reveals that ω-conotoxin MVIIB from *C. magus*, ω-conotoxin CVIB from *C. catus*, and ω-conotoxin CVIF were the shortest, consisting of only 25 amino acids. In contrast, ω-conotoxin GVIA from *C. geographus* and ω-conotoxin CVID from *C. catus* were the longest, comprising 73 amino acids each (Table 1).

3.2 Physicochemical properties of the ω-conotoxins

The physicochemical characteristics of the identified ω-conotoxins were examined using Expasy's ProtParam Tool, focusing on molecular weight, isoelectric point (pI), instability index (II), aliphatic index (AI), and the grand average of hydropathicity (GRAVY) (Table 2).

Table 1: Retrieved Protein Sequences.

SPECIES	ACCESSION NUMBER	PROTEIN NAME	LENGTH
C. geographus	P01522	ω-conotoxin GVIA	73
	P05483	ω-conotoxin GVIIA/GVIIB	29
C. magus	P05484	ω-conotoxin MVIIA	71
	P37300	ω-conotoxin MVIIC	29
	P05485	ω-conotoxin MVIIB	25
	Q26350	ω-conotoxin MVIID	29
C. striatus	P28880	ω-conotoxin SVIA	72
	P28881	ω-conotoxin SVIB	72
	Q9XZK2	ω-conotoxin SO-3	71
C. tulipa	P58915	ω-conotoxin TVIA	26
C. catus	P58920	ω-conotoxin CVID	73
	P58917	ω-conotoxin CVIA	71
	P58919	ω-conotoxin CVIC	26
	P58918	ω-conotoxin CVIB	25
	Q9N633	ω-conotoxin CVIE	66
	P0DQD4	ω-conotoxin CVIF	25

The isoelectric points (pI) of all identified ω-conotoxins were found to be above seven, with values ranging from 8.92 to 9.82, indicating their highly basic nature. This basicity is significant in understanding protein behavior, as the isoelectric point (pI) directly influences molecular interactions, particularly in complex formation where electrostatic forces between oppositely charged molecules play a critical role (Schuurmans *et al*., 2008). The pI also serves as a key determinant of protein solubility, subcellular localization, and potential interactions within the cellular environment (Moldoveanu & David, 2017; Lautenbach *et al*., 2021). Furthermore, it is essential in various biochemical applications, including protein isolation, separation, purification, and crystallization (Tokmakov *et al*., 201). The pronounced basicity of ω-conotoxins indicates that at physiological pH, these peptides typically carry a net positive charge. Such charge

enhances their interactions with negatively charged molecular targets, an important feature in their modulation of VGCCs (Akondi *et al*., 2014). This elevated pI is consistent with the functional requirements of ω-conotoxins as string electrostatic binding is necessary to effectively inhibit calcium channels, thereby blocking calcium ion influx and inducing paralysis in prey (Adams *et al*., 2011).

Table 2: Physicochemical Characteristics of the 16 ω-conotoxin from Selected Piscivorous *Conus* Species.

SPECIES	PROTEIN NAME	MOLECULAR WEIGHT	pI	II	AI	GRAVY
C. geographus	ω-conotoxin GVIA	7851.11	9.06	45.86 (Unstable)	74.79	-0.070
	ω-conotoxin GVIIA/GVIIB	3289.86	9.15	74.83 (Unstable)	26.90	-0.672
C. magus	ω-conotoxin MVIIA	7587.02	9.65	37.59 (Stable)	78.31	-0.023
	ω-conotoxin MVIIC	3070.63	9.55	43.46 (Unstable)	3.45	-0.921
	ω-conotoxin MVIIB	2625. 99	8.92	47.46 (Unstable)	4.00	-0.832
	ω-conotoxin MVIID	3103.53	9.48	27.93 (Stable)	3.45	-0.900
C. striatus	ω-conotoxin SVIA	7830.20	9.82	56.79 (Unstable)	70.42	-0.164
	ω-conotoxin SVIB	7741.15	9.50	45.35 (Unstable)	75.83	-0.158
	ω-conotoxin SO-3	7628.14	9.79	43.82 (Unstable)	75.63	-0.027
C. tulipa	ω-conotoxin TVIA	2804.17	8.67	105.40 (Unstable)	15.00	-0.585
C. catus	ω-conotoxin CVID	7748.19	9.35	28.84 (Stable)	80.14	0.073
	ω-conotoxin CVIA	7664.98	9.63	53.06 (Unstable)	68.73	-0.137
	ω-conotoxin CVIC	2790.29	9.13	88.93 (Unstable)	15.00	-0.681
	ω-conotoxin CVIB	2717.20	9.38	55.22 (Unstable)	4.00	-0.820
	ω-conotoxin CVIE	7053.20	9.80	56.18 (Unstable)	72.42	-0.209

ω-conotoxin CVIF	2672.10	9.18	64.12 (Unstable)	19.60	-0.616

The instability index (II) values of the ω-conotixuns showed considerable variation. Among the 16 identified proteins, only ω-conotoxins MVIIA (37.59), MVIID (27.93), and CVID (28.84) exhibited II values below 40, classifying them as stable. In contrast, the remaining 13 ω-conotoxins were considered unstable, with II values greater than 40. Such instability is commonly associated with the presence of specific dipeptide sequences that differ between stable and unstable proteins, potentially contributing to their propensity to degrade or misfold (Magliery, 2015). The aliphatic index (AI) of the selected ω-conotoxins also varied widely, ranging from 3.45 to 80.14. Notably, while ω-conotoxin MVIIC and MVIID from *C. magus* displayed the lowest AI value of 3.45, ω-conotoxin CVID from *C. catus* demonstrated the highest AI, reaching 80.14 The grand average hydropathy (GRAVY) value, which reflects a protein's hydrophilicity or hydrophobicity, was calculated for each ω-conotoxin. Typically, GRAVY values for most proteins fall within the range of -2 to +2. Results indicated that only ω-conotoxin CVID exhibited a positive GRAVY value of 0.073, classifying it as hydrophobic. In contrast, all remaining ω-conotoxins were hydrophilic, as indicated by their negative values.

3.3 Domains and Secondary Structures of the ω-conotoxins

The molecular domains of the ω-conotoxins were identified using the Pfam database, which revealed that seven of these peptides contain a characteristic domain associated with ω-conotoxins, corresponding to PROSITE entry PS60004. This domain, also documented under PROSITE entry PD0C60004, serves as a signature of the ω-conotoxin family and is commonly observed in approximately 30 presynaptic neurotoxins. In addition, seven ω-conotoxins were found to possess a domain from the Omega_toxin within the conotoxin family, underscoring the high degree of domain conservation among the ω-conotoxins analyzed. Interestingly, ω-conotoxin MVIIA and TVIA did not match any domains in the Pfam database, suggesting a possible sequence variation that distinguishes them from other ω-conotoxins.

Table 3. Domain Analysis of the ω-conotoxin from Selected Piscivorous *Conus* Species.

SPECIES	PROTEIN NAME	DOMAIN
C. geographus	ω-conotoxin GVIA	Omega_toxin
	ω-conotoxin GVIIA/GVIIB	OMEGA_CONOTOXIN

C. magus	ω-conotoxin MVIIA	N
	ω-conotoxin MVIIC	OMEGA_CONOTOXIN
	ω-conotoxin MVIIB	OMEGA_CONOTOXIN
	ω-conotoxin MVIID	OMEGA_CONOTOXIN
C. striatus	ω-conotoxin SVIA	Omega_toxin
	ω-conotoxin SVIB	Omega_toxin
	ω-conotoxin SO-3	Omega_toxin
C. tulipa	ω-conotoxin TVIA	N
C. catus	ω-conotoxin CVID	Omega_toxin
	ω-conotoxin CVIA	Omega_toxin
	ω-conotoxin CVIC	OMEGA_CONOTOXIN
	ω-conotoxin CVIB	OMEGA_CONOTOXIN
	ω-conotoxin CVIE	Omega_toxin
	ω-conotoxin CVIF	OMEGA_CONOTOXIN

The secondary structure components, including α-helix, extended strand, random coil, and beta turns, of the ω-conotoxins from selected piscivorous cone snails were retrieved from SOPMA. Among these ω-conotoxins, four exhibited the most α-helix content, specifically *C. striatus* ω-conotoxin SO-3 [38 (53.52%)] and SVIA [37 (51.39%)], *C. geographus* ω-conotoxin GVIA [36 (49.32%)], and *C. catus* ω-conotoxin CVID [35 (47.95%)]. On the contrary, six ω-conotoxins lacked α-helix in their sequences, including *C. magus* ω-conotoxin MVIIC, MVIIB, *C. tulipa* ω-conotoxin TVIA, *C. catus ω*-conotoxin CVIC, CVIB, and CVIF. Additionally, ω-conotoxin SVIA from *C. striatus* featured the highest number of β-strands [7 (9.72%)], while ω-conotoxin GVIIA from *C. geographus* and ω-conotoxin TVIA from *C. tulipa* lacked any β-strands in their sequences. Moreover, ω-conotoxin SVIB from *C. striatus*, ω-conotoxin GVIA from *C. geographus*, and ω-conotoxins CVIA, CVIE, and CVID from *C. catus* had the highest proportion of random coils in their sequences, with percentages of 35 (48.61%), 35 (47.95%), 36 (50.70%), 33 (50.00%), and 33 (45.21%), respectively. In contrast, ω-conotoxin CVIC and CVIB from *C. catus* exhibited the lowest random coil content, with only 12 (46.15%) and 12 (48.00%), respectively. Furthermore, concerning the presence of β-turns in each protein sequence, *C. catus* ω-conotoxin CVIC and CVIB had the highest number of β-turns, with 12 (30.77%) and 12 (32.00%),

respectively, while *C. tulipa* ω-conotoxin TVIA did not exhibit any β-turns in its sequence.

Table 4. Predicted Secondary Structural Arrangement of the ω-conotoxin from Selected Piscivorous *Conus* Species.

SPECIES	PROTEIN NAME	ALPHA-HELIX	BETA STRAND	RANDOM COIL	BETA TURN
C. geographus	ω-conotoxin GVIA	36 (49.32%)	0	35 (47.95%)	2 (2.74%)
	ω-conotoxin GVIIA/GVIIB	2 (6.90%)	4 (13.79%)	16 (55.17%)	7 (24.14%)
C. magus	ω-conotoxin MVIIA	31 (43.66%)	6 (8.45%)	28 (39.44)	6 (8.45%)
	ω-conotoxin MVIIC	0	5 (17.24%)	17 (58.62%)	7 (24.14%)
	ω-conotoxin MVIIB	0	4 (16.00%)	17 (68.00%)	4 (16.00%)
	ω-conotoxin MVIID	2 (6.90%)	5 (17.24%)	16 (55.17%)	6 (20.69%)
C. striatus	ω-conotoxin SVIA	37 (51.39%)	7 (9.72%)	26 (36.11%)	2 (2.78%)
	ω-conotoxin SVIB	29 (40.28%)	3 (4.17%)	35 (48.61%)	5 (6.94%)
	ω-conotoxin SO-3	38 (53.52%)	2 (2.82%)	29 (40.85%)	2 (2.82%)
C. tulipa	ω-conotoxin TVIA	0	0	26 (100%)	0
C. catus	ω-conotoxin CVID	35 (47.95%)	2 (2.74%)	33 (45.21%)	3 (4.11%)
	ω-conotoxin CVIA	29 (40.85%)	4 (5.63%)	36 (50.70%)	2 (2.82%)
	ω-conotoxin CVIC	0	6 (23.08%)	12 (46.15%)	8 (30.77%)
	ω-conotoxin CVIB	0	5 (20.00%)	12 (48.00%)	8 (32.00%)
	ω-conotoxin CVIE	27 (40.91%)	4 (6.06%)	33 (50.00%)	2 (3.03%)
	ω-conotoxin CVIF	0	3 (12.00%)	17 (68.00%)	3 (20.00%)

Amino acid distribution analysis reveals that random coils were the most common secondary structure predicted by the percentage distribution of amino acids, followed by beta-turns, beta-

strands, and alpha-helices. The α-helix is typically composed of amino acids such as methionine (M), alanine (A), leucine (L), glutamate (E), and lysine (K), all of which contribute to its stable helical conformation (Leiro *et al*., 2017). In other conotoxins, such as α-conotoxins, residues within the α-helix are critical for receptor binding and functional interactions (Muttenthaler *et al*., 2011). In contrast, β-strands, often stabilized by tryptophan (W), tyrosine (Y), phenylalanine (F), valine (V), isoleucine (I), and threonine (T), are structurally distinct from α-helices. β-strands are firmly locked within the protein's tertiary structure, contributing to protein stability and specific binding interactions (Richardson & Richardson, 2002; Wang *et al*., 2020).

3.4 Construction of Homology Models for ω-conotoxin

The predicted three-dimensional structures of the ω-conotoxins, based on their sequences, were constructed using the SWISS-Model tool and the UCLA0DOE LAB server. The geenrated models as guided by the GMQE and QMEAN values exhibited a GMQE scores approaching 1 and QMEAN scores below 4.0, indicating high reliability.

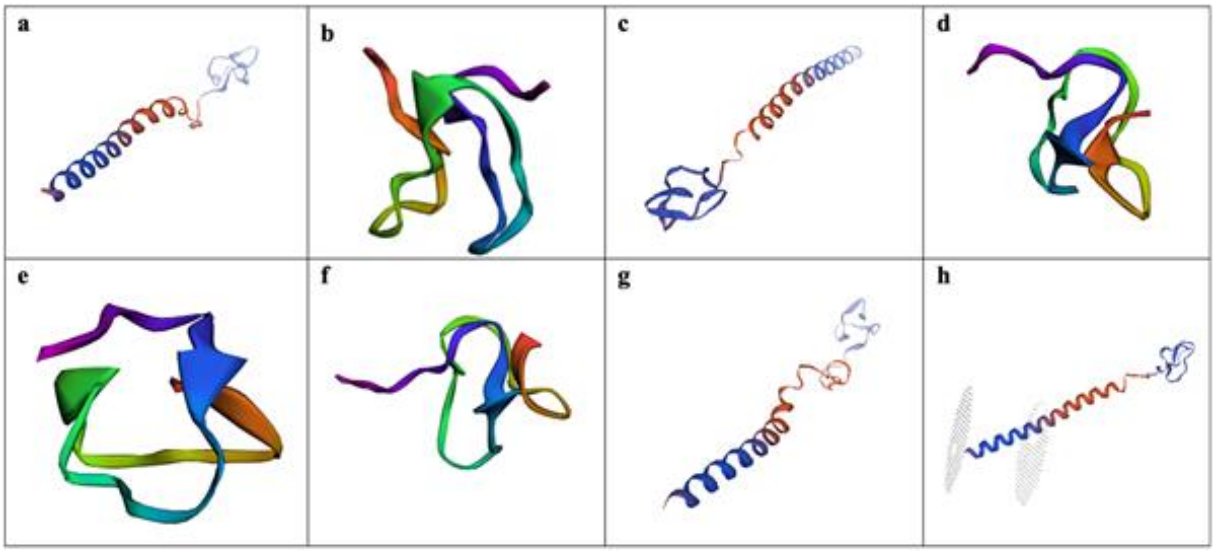

Figure 1. Homology models of ω-conotoxin from five selected piscivorous *Conus* species using SWISS-Model Tool and UCLA-DOE LAB. (a) ω-conotoxin GVIA, (b) ω-conotoxin GVIIA/CVIIB, (c) ω-conotoxin MVIIA, (d) ω-conotoxin MVIIC, (e) ω-conotoxin MVIIB, (f) ω-conotoxin MVIID, (g) ω-conotoxin SVIA, (h) ω-conotoxin SVIB.

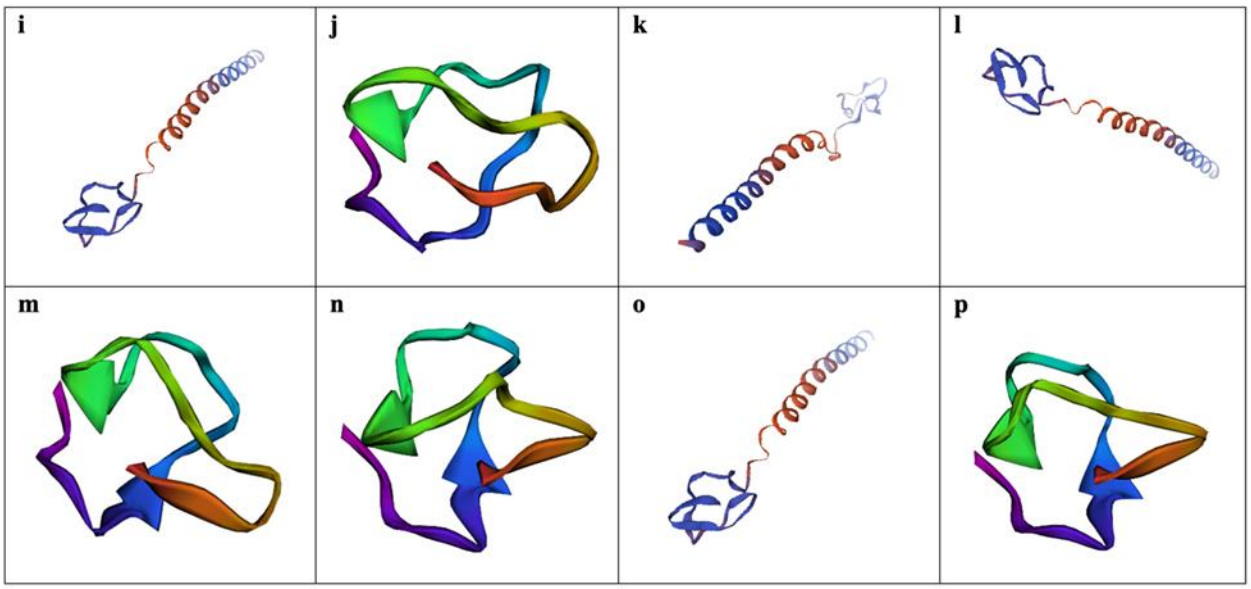

Figure 1: (continued). Homology models of ω-conotoxin from five selected piscivorous *Conus* species using SWISS-Model Tool and UCLA-DOE LAB. (i) ω-conotoxin SO-3, (j) ω-conotoxin TVIA, (k) ω-conotoxin CVID, (l) ω-conotoxin CVIA, (m) ω-conotoxin CVIC, (n) ω-conotoxin CVIB, (o) ω-conotoxin CVIE, and (p) ω-conotoxin CVIF

3.5 Validation of ω-conotoxin Models

Ramachandran plots were generated using the PDBsum webserver to assess the structural quality of the ω-conotoxin models, with the most favored regions highlighted in red. In these plots, glycine residues are represented by triangles, whereas all other amino acid residues are shown as squares. The analysis shows that ω-conotoxins MVIIC, MVIIB, TVIA, CVIA, CVIC, CVIB, and CVIF achieved high percentages of residues within favored regions—90.5%, 94.7%, 90.0%, 92.3%, 95.0%, 94.7%, and 100%, respectively (Table 5).

Table 5: Calculation and analysis of Ramachandran plots for the ω-conotoxin models of selected piscivorous Conus species.

SPECIES	PROTEIN NAME	RAMACHANDRAN PLOT	
		FAVORED REGION	DISALLOWED REGION
C. geographus	Omega-conotoxin GVIA	55 (84.6%)	0 (0.0%)
	Omega-conotoxin GVIIA/GVIIB	19 (82.6%)	0 (0.0%)
C. magus	Omega-conotoxin MVIIA	55 (85.9%)	0 (0.0%)
	Omega-conotoxin MVIIC	19 (90.5%)	0 (0.0%)
	Omega-conotoxin MVIIB	18 (94.7%)	0 (0.0%)

	Omega-conotoxin MVIID	19 (82.6%)	0 (0.0%)
C. striatus	Omega-conotoxin SVIA	48 (75.0%)	0 (0.0%)
	Omega-conotoxin SVIB	48 (75.0%)	0 (0.0%)
	Omega-conotoxin SO-3	57 (89.1%)	0 (0.0%)
C. tulipa	Omega-conotoxin TVIA	18 (90.0%)	0 (0.0%)
C. catus	Omega-conotoxin CVID	52 (78.8%)	1 (1.5%)
	Omega-conotoxin CVIA	60 (92.3%)	0 (0.0%)
	Omega-conotoxin CVIC	19 (95.0%)	0 (0.0%)
	Omega-conotoxin CVIB	18 (94.7%)	0 (0.0%)
	Omega-conotoxin CVIE	46 (78.0%)	0 (0.0%)
	Omega-conotoxin CVIF	19 (100.0%)	0 (0.0%)

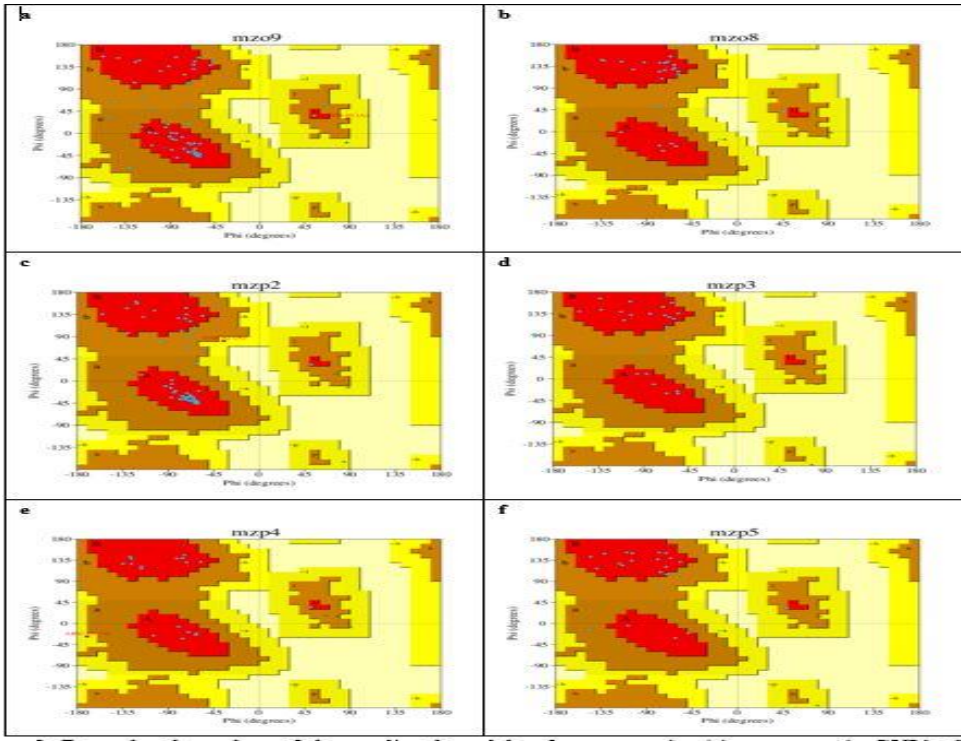

Figure 2: Ramachandran plots of the predicted models of ω-conotoxin. (a) ω-conotoxin GVIA, (b) ω-conotoxin GVIIA/CVIIB, (c) ω-conotoxin MVIIA, (d) ω-conotoxin MVIIC, (e) ω-conotoxin MVIIB, (f) ω-conotoxin MVIID.

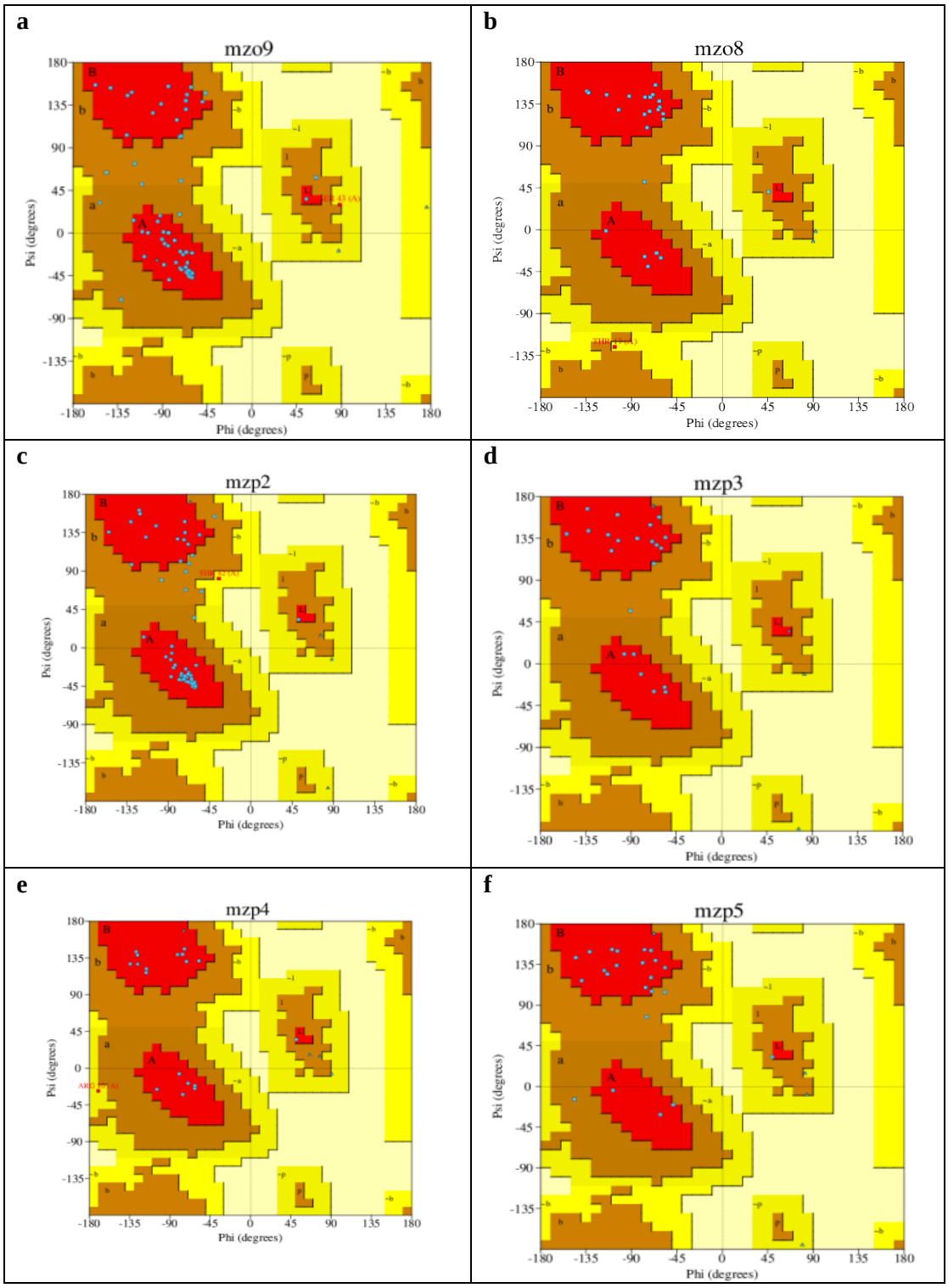

Figure 2: (continued) Ramachandran plots of the predicted models of ω-conotoxin. (a) ω-conotoxin GVIA, (b) ω-conotoxin GVIIA/CVIIB, (c) ω-conotoxin MVIIA, (d) ω-conotoxin MVIIC, (e) ω-conotoxin MVIIB, (f) ω-conotoxin MVIID.

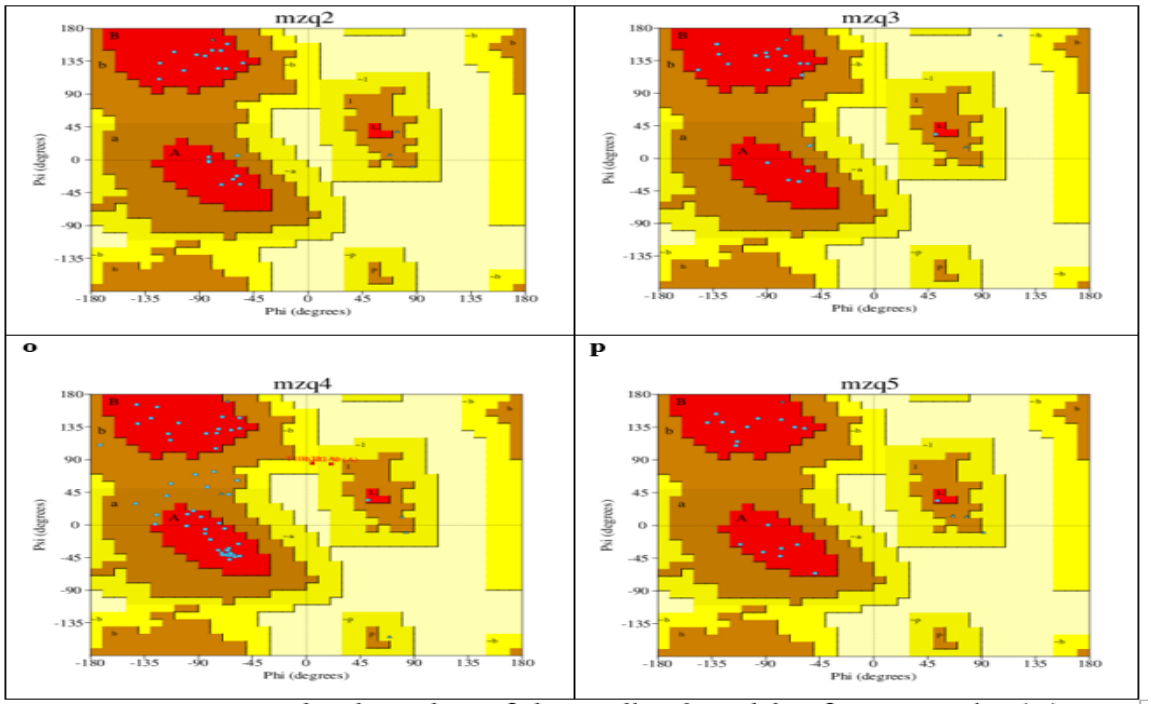

Figure 2: (continued) Ramachandran plots of the predicted models of ω-conotoxin. (m) ω-conotoxin CVIC, (n) ω-conotoxin CVIB, (o) ω-conotoxin CVIE, and (p) ω-conotoxin CVIF.

Figure 2. Ramachandran plots of the predicted models of ω-conotoxin. (a) ω-conotoxin GVIA, (b) ω-conotoxin GVIIA/CVIIB, (c) ω-conotoxin MVIIA, (d) ω-conotoxin MVIIC, (e) ω-conotoxin MVIIB, (f) ω-conotoxin MVIID. Figure 2 (continued). Ramachandran plots of the predicted models of ω-conotoxin. (e) ω-conotoxin MVIIB, (f) ω-conotoxin MVIID, (g) ω-conotoxin SVIA, (h) ω-conotoxin SVIB, (i) ω-conotoxin SO-3, (j) ω-conotoxin TVIA, (k) ω-conotoxin CVID, (l) ω-conotoxin CVIA,Figure 2 (continued). Ramachandran plots of the predicted models of ω-conotoxin. (m) ω-conotoxin CVIC, (n) ω-conotoxin CVIB, (o) ω-conotoxin CVIE, and (p) ω-conotoxin CVIF. These values indicate that these models possess high-quality structural conformations. In contrast, the remaining ω-conotoxins show less than 90% of residues within favored regions, suggesting lower quality for these models (Table 5), though these models do not have disallowed regions. Notably, while most ω-conotoxins display no residues in disallowed regions, ω-conotoxin CVID from C. catus exhibits one residue in the disallowed region. Identifying residues within disallowed regions is crucial for molecular modelers and structural biologists, as these regions may represent areas requiring refinement during protein modeling or fitting (Gopalakrishnan *et al*., 2007).

4. Discussion

In this study, 16 ω-conotoxins from five piscivorous *Conus* species were characterized through in silico analysis methods, and the findings of this study highlights the diversity, stability, and therapeutic potential within the ω-conotoxin family. The retrieved sequences

exhibited a broad length range from 25 to 37 amino acids. More notably, the ω-conotoxins MVIIB, CVIB, and CVIF were among the shortest conotoxins with 25 amino acids, while GIA and CVID were the longest consisting of 73 amino acids. These number of identified amino acids aligns with current research suggesting that conotoxins may have wider length ranges than the traditional 10-30 residues (Li *et al*., 2024), with the variation in length may correlate with varied structural motifs and functional conotoxin diversification. Physicochemical analysis revealed universally basic isoelectric points (pI 8.92-9.82), consistent with earlier findings in alpha-conotoxins and emphasizing their cationic nature in aqueous environments (Saguil *et al*., 2023). Only three peptides, MVIIA, MVIID, and CVID showed stability, suggesting that most of the studied ω-conotoxins may be inherently unstable, posing challenges in purification and manipulation. The aliphatic index (AI), ranged from ~3.5 in MVIIC/MVIID to ~80 in CVID. The high AI of CVID may suggest an enhanced thermostability, potentially advantageous for therapeutic applications under varying conditions. GRAVY values revealed hydrophilicity across most peptides, with only CVID being mildly hydrophobic. The hydrophilic nature promotes solubility, which is crucial for both experimental handling and drug delivery. Additionally, despite the hydrophilicity of most studied conotoxins, the conotoxin MVIIA (Ziconitide/Prialt) has been developed into an effective analgesic, demonstrating that solubility can be utilized without compromising bioactivity (Mansbach *et al*., 2019). Domain analysis indicated the presence of Pfam PF02950 in many of the sequences, which may reflect a conserved ω-conotoxin structural pattern and potential evolutionary linkage to SPOUT methyltransferase folds, such as conserved motifs that may facilitate ligand binding or structural folding. Secondary structure predictions through SOPMA also revealed that α-helices were most abundant in the toxins, whereas others lacked helical elements entirely. Random coils were also prevalent across the studied sequences, with β-strands and β-turns varying. These structural heterogeneities reflect the functional diversity of conotoxins, which target specific ion channels (Li *et al*., 2024). High-quality homology models, especially those with >90% of residues in the favored regions on the Ramachandran plots, such as MVIIB, CVIC, CVIB, CVIF, are indicating reliable structural predictions. One residue in a disallowed region in CVID underscores the need for cautious interpretation or further refinement. Reliable models aid in providing prospects for docking and rational design of conotoxin-based therapeutics. Recent in silico advances, such as deep learning frameworks like ConoDL, are capable of generating novel conotoxin-like sequences with plausible cysteine scaffolds and physicochemical congruence to natural peptides, offering an exciting avenue to expand the molecular space. Additionally, integrative machine learning approaches that incorporate post-transcriptional modification and structural

features can enhance prediction accuracy for conotoxin classes and targets with >90% accuracy.

5. Conclusion

This study explored the properties of ω-conotoxins from various piscivorous cone snail species, focusing on protein sequence characteristics, physicochemical profiles, structural domains, and secondary structures. Analysis revealed notable diversity in sequence length and physicochemical traits, particularly the high isoelectric points, which suggest the positively charged nature of these peptides. This feature likely facilitates their interaction with voltage-gated calcium channels, a central aspect of their functional role. Although most ω-conotoxins exhibited stability indices that signal inherent instability, posing a challenge for therapeutic applications, these limitations could potentially be overcome with advanced protein engineering techniques. Variability in aliphatic indices and hydropathy values indicated that higher aliphatic values may confer greater thermal stability, an advantageous property in drug development. Domain analysis emphasized conservation across ω-conotoxin domains, yet structural diversity was apparent, suggesting subtle adaptations in biological interactions. Homology models further supported reliable structural predictions, although refinement remains necessary for certain ω-conotoxins to meet optimal structural quality. Collectively, these findings suggest the therapeutic promise of ω-conotoxins as specialized inhibitors of VGCCs, with implications for novel treatments in pain management, neuroprotection, and related fields. While this study focused only on the selected piscivorous *Conus* species, it is important to do more research on other *Conus* species, as future research could explore ω-conotoxin in a broader range to uncover new structural variants. Given the instability indices observed, future studies should investigate methods like targeted mutagenesis or chemical modifications to enhance stability, making ω-conotoxins more suitable for clinical use. Exploring domain variations within the ω-conotoxin family and related conotoxins could also reveal unique structural features that contribute to their functional specificity. Such comparative analysis might also reveal evolutionary adaptations that enhance VGCC inhibition. Moreover, employing molecular docking, molecular dynamics simulations, and high-throughput screening methods could accelerate the identification of ω-conotoxins with optimal binding properties. This combined approach could support the design of derivatives with improved pharmacokinetics and pharmacodynamics.

References

Adams, D. J., Callaghan, B., & Géza Berecki. (2011). Analgesic conotoxins: block and G protein-coupled receptor modulation of N-type ($Ca_V2.2$) calcium channels. *British Journal of Pharmacology*, *166*(2), 486–500.

https://doi.org/10.1111/j.1476-5381.2011.01781.x

Akondi, K. B., Muttenthaler, M., Dutertre, S., Kaas, Q., Craik, D. J., Lewis, R. J., & Alewood, P. F. (2014). Discovery, synthesis, and structure–activity relationships of conotoxins. *Chemical Reviews*, *114*(11), 5815-5847.

Altier, C., Dale, C. S., Kisilevsky, A. E., Chapman, K., Castiglioni, A. J., Matthews, E. A., ... & Zamponi, G. W. (2007). Differential role of N-type calcium channel splice isoforms in pain. *Journal of Neuroscience*, *27*(24), 6363-6373.

Becker, S. and Terlau, H. (2008). Toxins from cone snails: Properties, applications and biotechnological production. *Applied Microbiology and Biotechnology*, *79*(1), pp. 1–9. doi:10.1007/s00253-008-1385-6.

Dutertre, S., Jin, A. H., Vetter, I., Hamilton, B., Sunagar, K., Lavergne, V., ... & Lewis, R. J. (2014). Evolution of separate predation-and defence-evoked venoms in carnivorous cone snails. *Nature communications*, *5*(1), 3521.

Gopalakrishnan,K., Sowmiya, G., Sheik, S. S., and Sekar, K. (2007). Ramachandran Plot on The Web (2.0). *Protein & Peptide Letters*, *14*(7), pp.669–671. doi:https://doi.org/10.2174/092986607781483912.

Hannon, H., & Atchison, W. (2013). Omega-Conotoxins as Experimental Tools and Therapeutics in Pain Management. *Marine Drugs*, *11*(3), 680–699. https://doi.org/10.3390/md11030680

Hendricks, J. R. (2018). Diversity and preserved shell coloration patterns of Miocene Conidae (Neogastropoda) from an exposure of the Gatun Formation, Colón Province, Panama. *Journal of Paleontology*, *92*(5), 804–837. https://doi.org/10.1017/jpa.2017.153

Jin, A.-H., Muttenthaler, M., Dutertre, S., Himaya, S. W. A., Kaas, Q., Craik, D. J., … Alewood, P. F. (2019). *Conotoxins: Chemistry and Biology. Chemical Reviews.* doi:10.1021/acs.chemrev.9b00207

Lage, O. M., Ramos, M. C., Calisto, R., Almeida, E., Vasconcelos, V., & Vicente, F. (2018). Current Screening Methodologies in Drug Discovery for Selected Human Diseases. *Marine Drugs*, 16(8), 279–279. https://doi.org/10.3390/md16080279

Li, R., Hasan, M. M., & Wang, D. (2024). In Silico Conotoxin Studies: Progress and Prospects. *Molecules*, *29*(24), 6061. https://doi.org/10.3390/molecules29246061

Magliery T. J. (2015). Protein stability: computation, sequence statistics, and

new experimental methods. *Current opinion in structural biology*, *33*, 161–168. https://doi.org/10.1016/j.sbi.2015.09.002

Mansbach, R., Travers, T., Mcmahon, B., Fair, J., & Gnanakaran, S. (2019). *Snails in Silico: A Review of Computational Studies on the Conotoxins*. https://doi.org/10.13140/RG.2.2.16966.73288

Moldoveanu, S.C. and David, V. (2017). Chapter 5 - Properties of Analytes and Matrices Determining HPLC Selection. *Selection of the HPLC Method in Chemical Analysis*, 189-230. doi:10.1016/B978-0-12-803684-6.00005-6.

Muttenthaler, M., B. Akondi, K., & F. Alewood, P. (2011). Structure-Activity Studies on Alpha-Conotoxins. Current Pharmaceutical Design, 17(38), 4226–4241. doi:10.2174/138161211798999384

Olivera, B. M. (2006). Conus peptides: biodiversity-based discovery and exogenomics. Journal of Biological Chemistry, 281(42), 31173-31177.

Olivera, B. M., Gray, W. R., Zeikus, R., McIntosh, J. M., Varga, J., Rivier, J., ... & Cruz, L. J. (1985). Peptide neurotoxins from fish-hunting cone snails. *Science*, *230*(4732), 1338-1343.

Puillandre, N., Bouchet, P., Duda, T. F., S. Kauferstein, Kohn, A. J., Olivera, B. M., Watkins, M., & Meyer, C. (2014). Molecular phylogeny and evolution of the cone snails (Gastropoda, Conoidea). *Molecular Phylogenetics and Evolution*, 78, 290–303. https://doi.org/10.1016/j.ympev.2014.05.023

Richardson, J. S., & Richardson, D. C. (2002). Natural β-sheet proteins use negative design to avoid edge-to-edge aggregation. *Proceedings of the National Academy of Sciences*, *99*(5), 2754–2759. https://doi.org/10.1073/pnas.052706099

Robinson, S. D., Safavi-Hemami, H., McIntosh, L. D., Purcell, A. W., Norton, R. S., & Papenfuss, A. T. (2014). Diversity of conotoxin gene superfamilies in the venomous snail, Conus victoriae. *PloS one*, *9*(2), e87648. https://doi.org/10.1371/journal.pone.0087648

Saguil, N., Currently, I., Caril, A., Lloyd, V., Paez, Adriene, M., Gonzales, J., Sofia, H., De Guzman, S. H., & Bantigue, P. C. (2023). In Silico Analysis And Homology Modeling Of Alpha-Conotoxin From Selected Vermivorous Conus Species. *Jilin Daxue Xuebao (Gongxueban)/Journal of Jilin University (Engineering and Technology Edition)*, *42*, 10–27.

https://doi.org/10.17605/OSF.IO/9MRVS

Sahay, A., Piprodhe, A., & Pise, M. (2020). In silico analysis and homology modeling of strictosidine synthase involved in alkaloid biosynthesis in catharanthus roseus. *Journal of Genetic Engineering and Biotechnology*, 18(1), doi:10.1186/s43141-020-00049-3

Tokmakov, A.A., Kurotani, A. and Sato, K.-I. (2021) 'Protein pi and intracellular localization', *Frontiers in Molecular Biosciences*, *8*. doi:10.3389/fmolb.2021.775736.

Wang, H., Logan, D. T., Danielsson, J., & Oliveberg, M. (2020). Exposing the distinctive modular behavior of β-strands and α-helices in folded proteins. *Proceedings of the National Academy of Sciences*, 117(46), 28775–28783. https://doi.org/10.1073/pnas.1920455117

Wang, Y., Zhang, H., Zhong, H., & Xue, Z. (2021). Protein domain identification methods and online resources. *Computational and structural biotechnology journal*, *19*, 1145–1153. https://doi.org/10.1016/j.csbj.2021.01.041

Waterhouse, A., Bertoni, M., Bienert, S., Studer, G., Tauriello, G., Gumienny, R., … Schwede, T. (2018). SWISS-MODEL: homology modelling of protein structures and complexes. *Nucleic Acids Research*, *46*(W1), W296–W303. doi:10.1093/nar/gky427